Highly Conjugated Side-Chain-Substituted Benzo[1,2-b:4,5-b′]dithiophene-Based Conjugated Polymers for Use in Polymer Solar Cells

ARTICLE *in* MACROMOLECULES · DECEMBER 2013

Impact Factor: 5.8 · DOI: 10.1021/ma402245t

9 AUTHORS, INCLUDING:

Chang Eun Song
Korea Research Institute of Chemical Technol…
30 PUBLICATIONS **358** CITATIONS
SEE PROFILE

Sang-Kyu Lee
Sookmyung Women's University
132 PUBLICATIONS **1,723** CITATIONS
SEE PROFILE

Won Suk Shin
Korea Research Institute of Chemical Technol…
110 PUBLICATIONS **2,108** CITATIONS
SEE PROFILE

Macromolecules

Article

pubs.acs.org/Macromolecules

Highly Conjugated Side-Chain-Substituted Benzo[1,2-*b*:4,5-*b*′]dithiophene-Based Conjugated Polymers for Use in Polymer Solar Cells

Ha-Seul Chung,[†] Woo-Hyung Lee,[†] Chang Eun Song,[‡] Yurim Shin,[†] Joonghan Kim,[†] Sang Kyu Lee,[§] Won Suk Shin,[§] Sang-Jin Moon,[§] and In-Nam Kang*[,†]

[†]Department of Chemistry, The Catholic University of Korea, Bucheon, Republic of Korea

[‡]Department of Materials Science and Engineering, KAIST, Daejeon 305-701, Republic of Korea

[§]Energy Materials Research Division, Korea Research Institute of Chemical Technology, Daejeon, Republic of Korea

Supporting Information

ABSTRACT: A series of novel benzo[1,2-*b*:4,5-*b*′]-dithiophene (BDT)-based conjugated polymers were synthesized using a Stille cross-coupling reaction. These polymers contained dithienyl thieno[3,4-*c*]pyrrole-4,6-dione (DTTPD) as an acceptor. Alkylthienylenevinylene thiophene side groups were introduced into the BDT units, and the solubility, absorption spectra, energy levels, charge transport, blend film morphology, and photovoltaic properties of the resulting polymer (poly[4,8-bis{2,2′-(5-ethylhexyl)-thienylenevinylenethiophene}benzo[1,2-*b*;3,4-*b*]dithiophene-2,6-diyl-*alt*-1,3-di(thien-5′-yl)-5-octyldodecyl[3,4-*c*]pyrrole-4,6-dione-2,2′-diyl], PBDTTVT-DTTPD) were investigated. In addition, an alkylthienyl-substituted BDT-based polymer (poly[4,8-bis(5-(2-ethylhexyl)thiophen-2-yl)benzo[1,2-*b*:4,5-*b*′]dithiophene-2,6-diyl-*alt*-1,3-di(thien-5′-yl)-5-octyldodecyl[3,4-*c*]pyrrole-4,6-dione-2,2′-diyl], PBDTT-DTTPD) was synthesized to compare the optoelectronic and photovoltaic properties of the polymers. The weight-averaged molecular weights (M_w) of PBDTT-DTTPD and PBDTTVT-DTTPD were found to be 41 000 and 58 100 Da, with polydispersity indices of 2.0 and 2.2, respectively. Photophysical studies revealed low bandgaps of 1.88 eV for PBDTT-DTTPD and 1.87 eV for PBDTTVT-DTTPD. The PBDTTVT-DTTPD thin film was able harvest a broad solar spectrum covering the range from 300 to 700 nm. Solution-processed field-effect transistors fabricated from these polymers displayed p-type organic thin film transistor characteristics. The field-effect mobilities of PBDTT-DTTPD and PBDTTVT-DTTPD were measured to be 3.2×10^{-3} and 1.8×10^{-3} cm^2 V^{-1} s^{-1}, respectively. A polymer solar cell device prepared using PBDTTVT-DTTPD as the active layer exhibited a power conversion efficiency (PCE) of 6.04% with a high open circuit voltage of 0.87 V under AM 1.5 G (100 mW/cm^2) conditions.

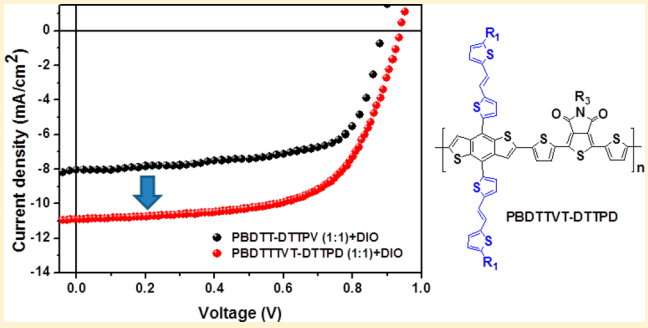

INTRODUCTION

In recent years, conjugated polymers have been intensively investigated for use in solution-processed polymer solar cells (PSCs) because they are flexible and enable low-cost device fabrication via solution processing.[1] Bulk heterojunction (BHJ) polymer solar cells based on a variety of blends of electron-donating conjugated polymers and electron-accepting fullerene derivatives have been tested in the effort to increase their power conversion efficiencies (PCEs).[2] Recently, significant progress has been made in this field, and the PCEs of PSCs have reached approximately 9.2% as a result of the development of new conjugated polymers and improvements in the control over the morphologies of bicontinuous interpenetrating electron donor/acceptor nanoscale networks.[3] Conjugated polymers that incorporate alternating donor and acceptor units provide relatively low bandgaps due to the introduction of intramolecular charge transfer (ICT) complexes.[4] Of the various donor units tested in donor−acceptor (D−A) systems, benzo[1,2-*b*:4,5-*b*′]dithiophene (BDT) is the most promising electron donor material for use in high-performance PSCs. Its large planar π-conjugated structure promotes facile $\pi-\pi$ stacking, improves the hole mobility, and facilitates the introduction of alkyl or aryl side chains that can be used to control the solubility and optical properties of the polymer.[5] Moreover, the optoelectronic properties of BDT-based D−A polymers can be tuned by introducing a variety of substituents onto the central phenyl rings of the BDT units.[6] Recently, several research groups have introduced alkylthienyl groups onto the BDT units and achieved PCEs of up to 7% as a result of a reduction in the highest occupied molecular orbital (HOMO) energy level and the broadening of the absorption spectrum. For example, Hou et al. reported the development of

Received: October 30, 2013
Revised: December 16, 2013
Published: December 31, 2013

novel alkylthienyl-substituted BDT building blocks.[7] The introduction of alkylthienyl substituents onto the BDT units of D−A polymers was found to extend the conjugation between the BDT building blocks, enhance the hole mobility, and decrease the HOMO energy level compared to the level in a dialkoxy-substituted BDT analogue.[7] Stefan et al. reported the synthesis of a novel BDT-based copolymer bearing six alkyl-substituted bithienyl side groups that improved the solubility of the polymer and provided a broader absorption spectrum in the visible region.[8] Hou et al. reported the synthesis and photophysical properties of the polythiophenes and poly(thienylene vinylenes) containing thienylene vinylene side groups; their absorption spectra showed a broad plateau in the visible region.[9] In this study, we synthesized a new polymer (PBDTTVT-DTTPD) with alternating alkylthienylenevinylene thiophene (TVT) side groups incorporated into the BDT donor units and dithienyl thieno[3,4-*c*]pyrrole-4,6-dione (DTTPD) acceptor units. By adding the highly conjugated TVT side groups to the BDT building blocks of the polymers, we expected the absorption band to broaden, thereby improving the short circuit current (J_{sc}). The optical, electrochemical, and photovoltaic properties of these polymers were also investigated. As a control, the alkylthienyl-substituted BDT-based DTTPD copolymer (PBDTT-DTTPD) was synthesized using the same polymerization method. The synthetic routes for the monomers and the new BDT-based D−A polymers are outlined in Schemes 1 and 2.

Scheme 1. Synthetic Routes for the BDT Monomers

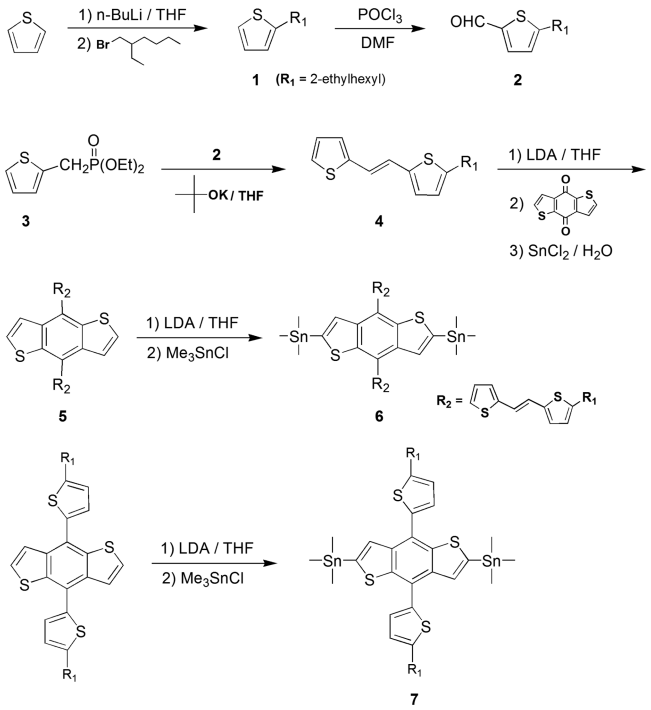

RESULTS AND DISCUSSION

Synthesis and Characterization. As shown in Scheme 1, compound **4** was prepared from compound **3** and 2-formyl-5-(2-ethyl)hexylthiophene in good yield (74%) via the Horner−Wadsworth−Emmons reaction and was found to assume the trans configuration, as determined using ^{1}H NMR and FT-IR spectroscopy. The out-of-plane bending vibration of the vinyl C−H group in compound **4** produces a peak at 930 cm^{-1}, which means that the vinyl group in the compound **4** is a trans configuration. This result is in good agreement with the appearance of the FT-IR spectra of compound **6** (the distannyl monomer) and PBDTTVT-DTTPD, which are shown in Figure 1. As a comparison, the FT-IR spectrum of PBDTT-DTTPD was measured, but no peak was observed in this region. PBDTT-DTTPD and PBDTTVT-DTTPD were obtained via a Stille coupling reactions between compounds **7** and **8** and compounds **6** and **8**, respectively (Scheme 2). The weight-average molecular weights (M_w) of PBDTT-DTTPD and PBDTTVT-DTTPD were determined by gel permeation chromatography (GPC) using a polystyrene standard in a chloroform eluting solvent. These values were found to be 41 000 (PDI = 2.0) and 58 100 (PDI = 2.2), respectively. The 2-octyldodecyl and 2-ethylhexyl substituents were found to impart the appropriate solubility to the polymers in common organic solvents, such as toluene, chloroform, and chlorobenzene. Solutions of the polymers formed good thin films. The thermal stabilities of the polymers were analyzed by thermogravimetric analysis (TGA). The decomposition temperatures (T_d) at 5% weight loss of PBDTT-DTTPD and PBDTTVT-DTTPD were 419 and 334 °C, respectively, indicating that alkylthienyl groups are more stable than alkylthienylenevinylene thiophene groups (Figure S1). Differential scanning calorimetry (DSC) measurements of the polymers found no significant thermal transitions. The polymerization results of the synthesized polymers are summarized in Table 1.

Optical and Electrochemical Properties. The UV−vis absorption spectra of PBDTT-DTTPD and PBDTTVT-DTTPD in solution and in the film state are shown in Figure 2. The absorption maxima (λ_{max}) of PBDTT-DTTPD and PBDTTVT-DTTPD in solution were at 557 and 570 nm, whereas the absorption peaks in the thin films were 556 and 564 nm, respectively. The λ_{max} of PBDTTVT-DTTPD was red-shifted by approximately 10 nm with respect to PBDTT-DTTPD in the solution and film states, possibly because the alkylthienylenevinylene thiophene (TVT) side groups in PBDTTVT-DTTPD increased the effective conjugation length to a greater extent than did the alkylthienyl groups in PBDTT-DTTPD. The UV−vis spectrum of the PBDTTVT-DTTPD thin film displayed two λ_{max} at 400 and 570 nm and a shoulder peak at 610 nm. The absorption maximum at the shorter wavelength (400 nm) was attributed to the BDT units bearing conjugated TVT side groups, which is well consistent with absorption maximum of the BDT monomer (compound **6**) in solution state (Figure 2a), whereas the absorption band at the longer wavelength was attributed to intramolecular charge transfer (ICT) between the BDT donor and the DTTPD acceptor. The absorption bands of PBDTTVT-DTTPD were slightly red-shifted and broadened compared to the bands of PBDTT-DTTPD. PBDTTVT-DTTPD exhibited the strong hyperchromic effect in the whole absorption range. Especially, the absorption intensity of PBDTTVT-DTTPD at 400 nm was significantly higher than that of the alkylthienyl-substituted polymer (PBDTT-DTTPD). The value of absorption coefficients (α) for PBDTTVT-DTTPD was a factor of 4 higher (7.1×10^4 cm^{-1}) than that of PBDTT-DTTPD (1.8×10^4 cm^{-1}) at 400 nm (Figure 2b). These drastic increase of absorption intensity for PBDTTVT-DTTPD at short wavelength (~400 nm) was attributed to the additional BDT monomer's (compound **6**) absorption because these additional

dx.doi.org/10.1021/ma402245t | Macromolecules 2014, 47, 97−105

Scheme 2. Synthetic Routes for PBDTT-DTTPD and PBDTTVT-DTTPD

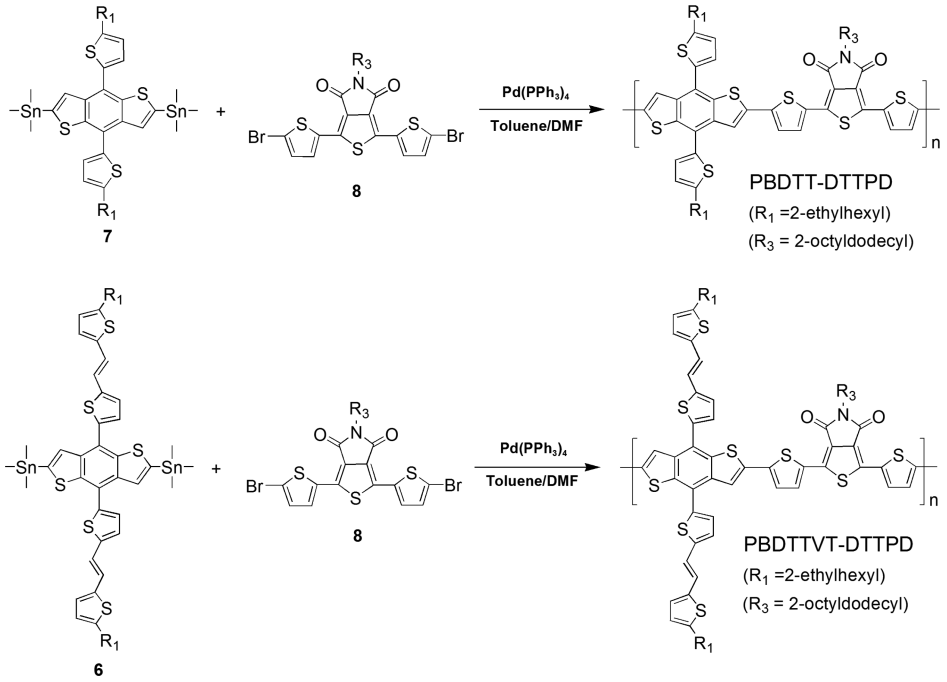

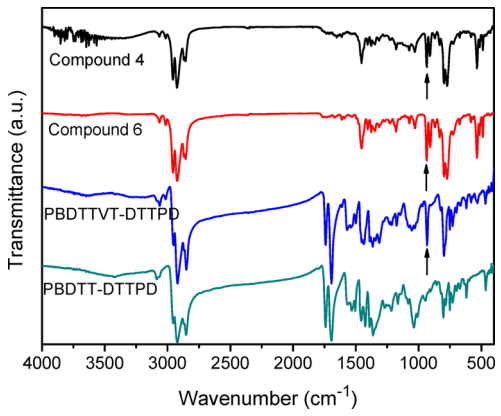

Figure 1. FT-IR spectra of compounds **4**, **6**, PBDTT-DTTPD, and PBDTTVT-DTTPD.

Table 1. Molecular Weights and Thermal Stabilities of PBDTT-DTTPD and PBDTTVT-DTTPD

polymer	M_n (g/mol)	M_w (g/mol)	PDI	T_d[a] (°C)
PBDTT-DTTPD	20.0K	41.0K	2.0	419
PBDTTVT-DTTPD	25.3K	58.1K	2.3	334

[a]Decomposition temperature at 5% weight loss.

chromophores (TVT groups) in PBDTTVT-DTTPD increase the absorption intensity at short wavelength. Moreover, the absorption intensity of PBDTTVT-DTTPD (7.5×10^4 cm^{-1}) at 550 nm was approximately 1.4 times higher than that of PBDTT-DTTPD (5.5×10^4 cm^{-1}). This increase is not well understood yet, but we guess that this behavior could originate from the difference of electron-donating ability of the donor parts in the polymers (BDTT and BDTTVT), possibly because the HOMO orbitals of BDTT and BDTTVT donor units exhibited different π-electron delocalization from each other (see Computational Study section). The onsets of the optical absorptions of the PBDTT-DTTPD and PBDTTVT-DTTPD

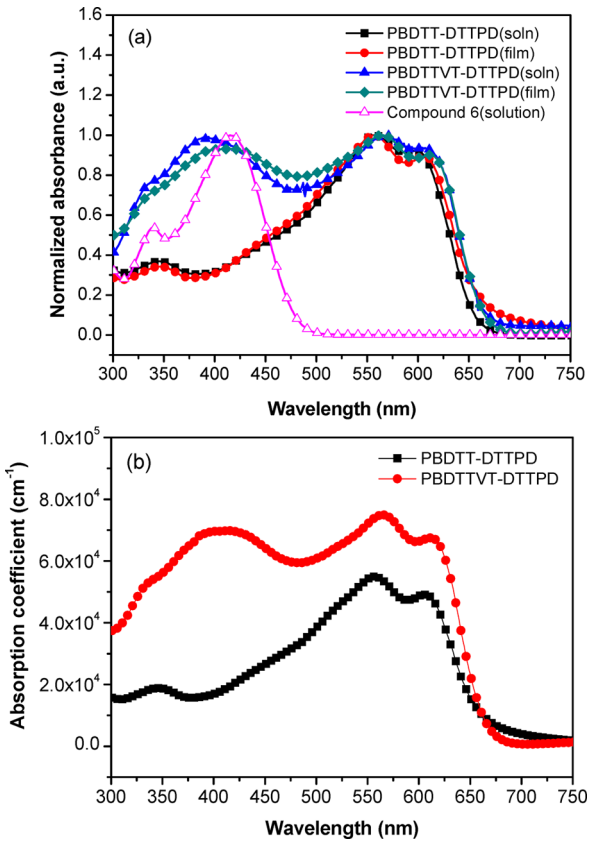

Figure 2. (a) UV–vis absorption spectra of PBDTT-DTTPD and PBDTTVT-DTTPD in a chloroform solution and in a thin film state and (b) absorption coefficients of the polymer films.

films were found to be 660 nm (E_g = 1.88 eV) and 663 nm (E_g = 1.87 eV), respectively.

The HOMO levels of the polymer films were calculated from cyclic voltammetry (CV) measurements using the equation

dx.doi.org/10.1021/ma402245t | Macromolecules 2014, 47, 97–105

Table 2. UV−vis Maximum Absorption Wavelength (λ_{max}), Bandgap Energy (E_g), and Ionization Potential (E_{HOMO}) of PBDTT-DTTPD and PBDTTVT-DTTPD

						mobility ($cm^2/(V\ s)$)	
polymer	solution[a] (λ_{max}, nm)	film (λ_{max}, nm)	E_g (eV)	E_{HOMO} (eV)	E_{LUMO}[d] (eV)	FET	SCLC
PBDTT-DTTPD	347, 557, 600	347, 556, 602	1.88[b] (1.93)[c]	−5.43	−3.55	3.2×10^{-3}	4.9×10^{-5}
PBDTTVT-DTTPD	389, 570, 612	410, 564, 613	1.87[b] (1.81)[c]	−5.40	−3.53	1.8×10^{-3}	1.3×10^{-5}

[a]Measurements performed in chlorobenzene. [b]Estimated from the onset of the absorption of the thin solid film ($E_g = 1240/\lambda_{onset}$ eV). [c]Data from the quantum chemical calcuation. [d]Calculated from the optical bandgap energy.

$E_{HOMO} = -(E_{ox} + 4.8)$ eV, where E_{ox} is the onset oxidation potential relative to the ferrocene external standard (Figure S2). The HOMO levels of the polymer films exhibited a relatively low-lying HOMO energy level of −5.43 eV for PBDTT-DTTPD and −5.40 eV for PBDTTVT-DTTPD, indicating that similar V_{oc} values were expected for the two resulting polymer solar cell devices. The optical bandgaps of PBDTT-DTTPD and PBDTTVT-DTTPD were determined from the absorption onsets and were found to be 1.88 and 1.87 eV, respectively. The calculated lowest unoccupied molecular orbital (LUMO) levels of the PBDTT-DTTPD and PBDTTVT-DTTPD thin films were found to be −3.55 and −3.53 eV, respectively, which were higher (by about 0.7 eV) than the value obtained for the $PC_{71}BM$ ([6,6]-phenyl C_{71}-butyric acid methyl ester) acceptor (−4.30 eV), suggesting that charge transfer from the polymers to $PC_{71}BM$ was allowed. The optical and electrochemical properties of the polymers are summarized in Table 2.

Computational Study. All molecular structures of PBDTT-DTTPD and PBDTTVT-DTTPD were optimized using density functional theory (DFT) calculations. Subsequent harmonic vibrational frequency calculations were performed on the optimized molecular structures to identify a minimum-energy structure. We used the recently developed MN12-SX functional as DFT exchange-correlation functional.[10] The 6-31G(d) basis sets were used for all atoms. Because of the computational time, trimers were considered as the polymers. All calculations were carried out using the Gaussian09 program.[11] To simplify the calculations, 2-ethylhexyl and 2-octyldodecyl groups were replaced by ethyl and isobutyl groups, and three repeating units of each polymer were subjected to the calculations (Figure S3). In Figure S3, the electron density distributions of the HOMO orbitals for PBDTT-DTTPD are distributed in the polymer backbone, while HOMO orbitals for PBDTTVT-DTTPD are localized at BDTTVT donor units. The LUMO orbitals of the polymers are mainly located at the electron-withdrawing DTTPD units. Moreover, the electron density distributions in HOMO levels of all polymers are delocalized onto the side substituents (alkylthienyl and TVT groups) in BDT units, indicating that the π electrons can be easily delocalized in the BDT units as a result of introducing of the conjugated side groups. From these results, the π electrons can be delocalized better in TVT side groups, which may be due to the relatively longer conjugation length of TVT side groups. The bandgap energy of PBDTTVT-DTTPD model compound was slightly smaller than that of and PBDTT-DTTPD, and the result was consistent with the measured optical bandgap energies of the polymers.

Field-Effect Transistor and Space-Charge Limited Current Characteristics. The effects of the shape and position of a side chain on the electrical transport properties of the resulting polymers were examined by measuring the organic field-effect transistor (OFET) mobility. The field-effect carrier mobilities of the polymers were investigated by fabricating thin film transistors with a bottom-contact geometry using Au electrodes. The FET characteristics were determined under ambient conditions, and no precautions were taken to insulate the materials or devices from exposure to air, moisture, or light. The field-effect mobility was calculated according to the equation[12]

$$\text{saturated regime } (V_D > V_G):\ I_D = (W/2L)\mu C_i(V_G - V_T)^2$$

where I_D is the drain current in the saturated regime, W and L are the channel width and length, respectively, μ is the field-effect mobility, C_i is the capacitance per unit area of the gate dielectric layer, and V_G and V_T are the gate and threshold voltages, respectively. The results are plotted in Figure 3 and Figure S4. PBDTT-DTTPD and PBDTTVT-DTTPD exhibit typical p-type organic semiconductor characteristics with hole mobilities of 3.2×10^{-3} and 1.8×10^{-3} $cm^2\ V^{-1}\ s^{-1}$, respectively. The mobility of PBDTT-DTTPD was slightly higher than that of PBDTTVT-DTTPD, suggesting that

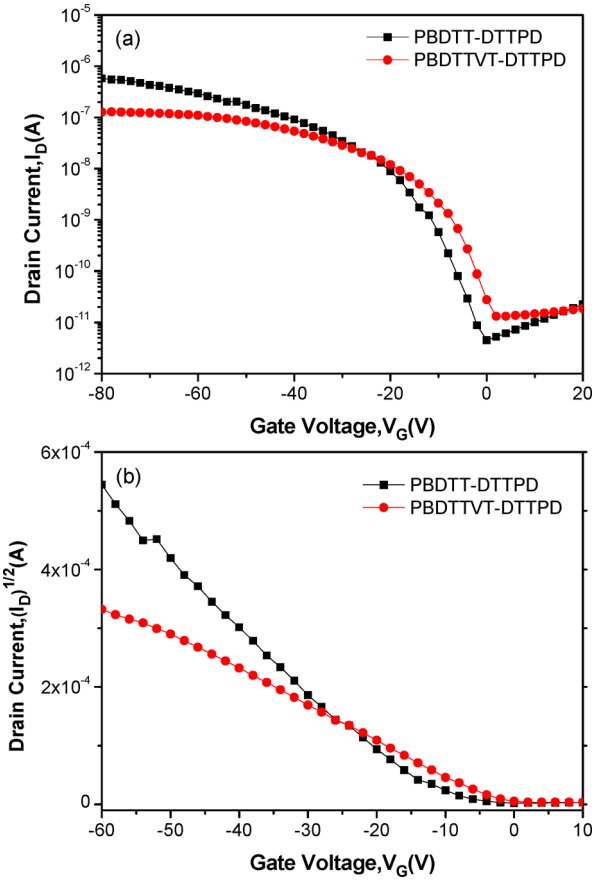

Figure 3. (a) I_D-V_G and (b) $(I_D)^{1/2}-V_G$ characteristics of the polymer FET devices prepared with an OTS-modified surface; $V_{DS} = -60$ V.

dx.doi.org/10.1021/ma402245t | Macromolecules 2014, 47, 97−105

polymer chain packing in PBDTT-DTTPD was better than that in PBDTTVT-DTTPD.

OFET devices can measure the charge transport to horizontal direction. We measured the hole mobilities of the polymer thin films using a space-charge limited current (SCLC) method to investigate the vertical carrier transport properties of the organic photovoltaic (OPV) devices. To obtain the SCLC curves, the hole-only devices were fabricated with the structure of ITO/PEDOT:PSS/polymers/Au, and the mobilities were calculated using the Mott–Gurney equation.[13] The voltage–current density curves of the fabricated hole-only devices of the polymers are shown in Figure S5. The measured SCLC mobilities of the PBDTT-DTTPD and PBDTTVT-DTTPD films were 4.9×10^{-5} and 1.3×10^{-5} $cm^2/(V\ s)$, respectively, which shows a similar trend to the FET mobilities of the polymer films.

Organic Photovoltaic Characteristics. The photovoltaic properties of PBDTT-DTTPD and PBDTTVT-DTTPD were measured in devices prepared with the general structure ITO/PEDOT:PSS/Polymer:$PC_{71}BM$ ([6,6]-phenyl C_{71}-butyric acid methyl ester)/LiF/Al. The device fabrication steps, characterization protocols, and results are summarized in Figure 4 and

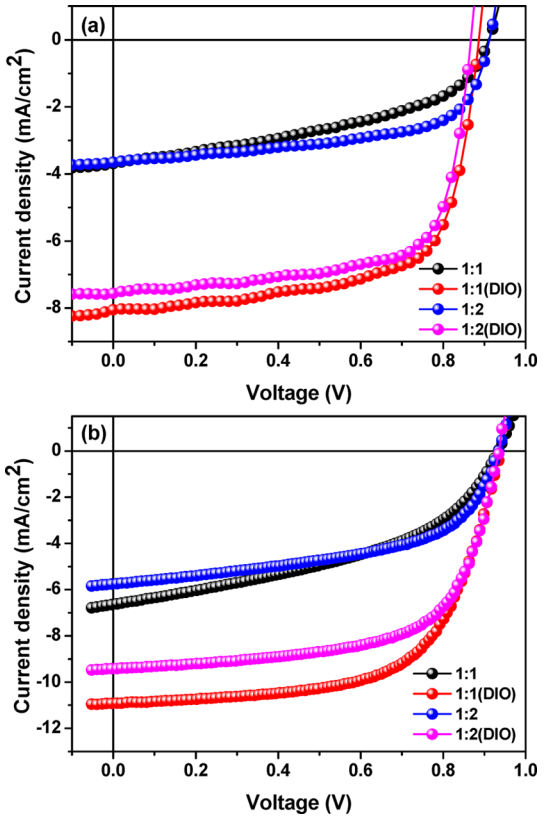

Figure 4. *J–V* characteristics of the (a) PBDTT-DTTPD/PCBM and (b) PBDTTVT-DTTPD/PCBM devices.

Table 3. The maximum power conversion efficiencies (PCEs) of the PBDTT-DTTPD and PBDTTVT-DTTPD devices were found to be 4.82% and 6.04%, respectively. The addition of 1,8-diiodooctane (DIO) to the blend solution was found to more than double the PCEs of the devices and to result in a much higher J_{sc} value. The open circuit voltage (V_{oc}) values, which are related to the differences between the HOMO levels of the donor polymers and the LUMO levels of the acceptor (PCBM), of the DIO-processed PBDTT-DTTPD:PCBM (1:1) and PBDTTVT-DTTPD:PCBM (1:1) devices were found to be 0.89 and 0.87 V, respectively. Theoretical achievable V_{oc} of our OPV devices could be calculated according to the equation[14]

$$V_{oc} = (1/e)(|E^{donor}\mathrm{HOMO}| - |E^{PCBM}\mathrm{LUMO}|) - 0.3\ \mathrm{V}$$

where e is the elementary charge and using −4.2 eV for the PCBM lowest occupied molecular orbital (LUMO) energy.[13] The theoretical V_{oc} values of the DIO-processed PBDTT-DTTPD:PCBM (1:1) and PBDTTVT-DTTPD:PCBM (1:1) devices were 0.93 and 0.90 V. The experimental V_{oc} values of the polymer devices were similar, in good agreement with the theoretical values. Moreover, the short circuit current (J_{sc}) value of the DIO-processed PBDTTVT-DTTPD device (10.9 mA/cm^2) was higher than the value of the DIO-processed PBDTT-DTTPD device (8.05 mA/cm^2). We believe that this high short circuit currents of the PBDTTVT-DTTPD devices could potentially have resulted from the enhanced light absorption properties (the bandgap profile and the optical absorption coefficients). The light absorption bandwidth of PBDTTVT-DTTPD (1.87 eV) was found to be slightly larger than that of PBDTT-DTTPD (1.88 eV); however, this difference was negligible in its effects on the device performance. The larger optical absorption coefficient of PBDTTVT-DTTPD relative to PBDTT-DTTPD, on the other hand, was significant at shorter wavelengths (350–500 nm). Surprisingly, the hole mobility of PBDTT-DTTPD was slightly higher than that of PBDTTVT-DTTPD, in contradiction with the PCE values of the polymer solar cells. The high J_{SC} of the PBDTTVT-DTTPD device appeared to have resulted primarily from the improved optical absorption coefficients. It should be noted that the incorporation of the conjugated TVT side groups into the BDT units significantly increased the absorption intensity at shorter wavelengths, thereby enhancing the J_{sc} and PCE values of the PBDTTVT-DTTPD solar cell devices.

Film surface morphology plays a key role in the efficiency of a bulk heterojunction polymer solar cell. Atomic force microscopy (AFM) images of the surface morphologies of each solar cell device were collected (Figure 5). In general, nanoscale phase separation is required to overcome the short exciton diffusion length (approximately 10 nm) of the donor polymers and provide efficient charge separation.[16] The root-mean-square (rms) roughness of PBDTT-DTTPD:PCBM (1:1) and PBDTTVT-DTTPD:PCBM (1:1) films were 4.7 and 3.6 nm for without DIO, whereas that of PBDTT-DTTPD:PCBM (1:1) and PBDTTVT-DTTPD:PCBM (1:1) films were 1.95 and 1.34 nm for with DIO, respectively. As can be seen in Figure 5, the PBDTTVT-DTTPD:PCBM (1:1) film showed smaller phase separations of polymer-PCBM domains than those of PBDTT-DTTPD:PCBM (1:1) film, which accounted for low rms roughness value and the high photocurrent density in the PBDTTVT-DTTPD:PCBM (1:1) film. In contrast, relatively high levels of phase separation were observed in the PBDTT-DTTPD:PCBM (1:1) film, which reduced the area for charge separation, leading to a low photocurrent. The dramatic differences between the device performances prepared with or without the DIO additive were most likely due to differences in the blend morphology. The AFM images clearly revealed the presence of large domains in the blend films prepared using chlorobenzene; these large domains would diminish exciton migration to the donor/acceptor interface and are not favorable for charge separation.

dx.doi.org/10.1021/ma402245t | Macromolecules 2014, 47, 97–105

Table 3. PSC Performances of the Polymer/$PC_{71}BM$ Devices

polymer	ratio	film thickness (nm)	J_{sc} [mA/cm^2]	V_{oc} [V]	FF	PCE [%]
PBDTT-DTTPD	1:1	68	3.69	0.91	0.44	1.49
	1:1[a]	72	8.05	0.89	0.68	4.82 (4.74)[b]
	1:2	70	3.65	0.91	0.59	1.96
	1:2[a]	74	7.56	0.87	0.69	4.55
PBDTTVT-DTTPD	1:1	72	6.64	0.91	0.45	2.72
	1:1[a]	74	10.90	0.87	0.63	6.04 (5.97)[b]
	1:2	68	5.75	0.91	0.53	2.79
	1:2[a]	75	9.42	0.87	0.64	5.26

[a]3% DIO additive (v/v). [b]Average PCE value for five devices.

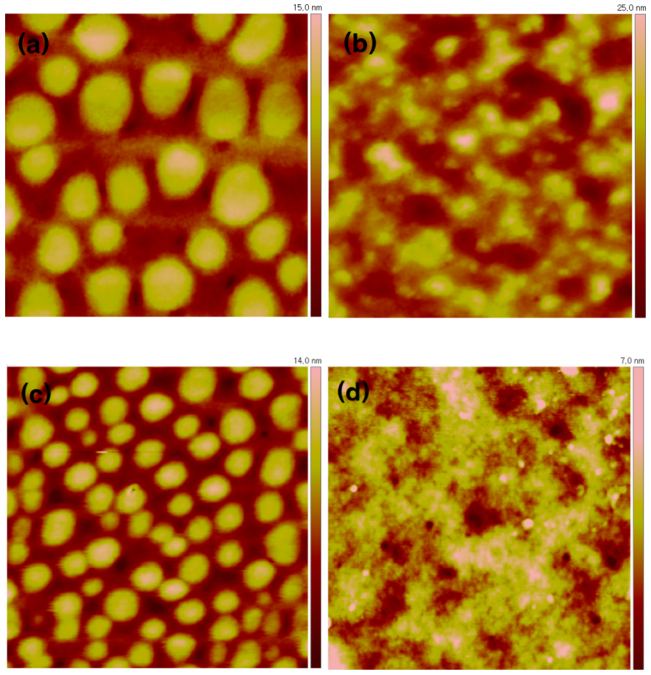

Figure 5. AFM tapping-mode height images of (a) PBDTT-DTTPD/PCBM (1:1), (b) PBDTT-DTTPD/PCBM (1:1) + DIO, (c) PBDTTVT-DTTPD/PCBM (1:1), and (d) PBDTTVT-DTTPD/PCBM (1:1) + DIO. Scan size was 2 μm × 2 μm.

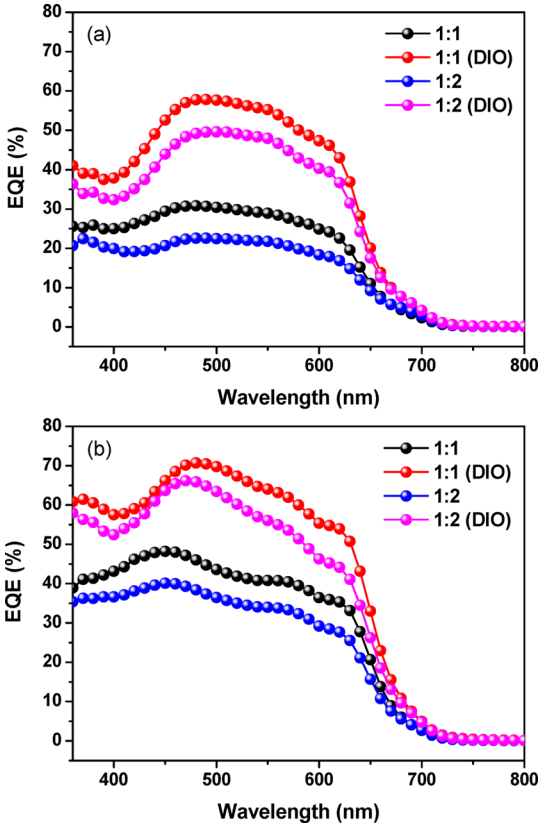

Figure 6. External quantum efficiency of the PBDTT-DTTPD/$PC_{71}BM$ and PBDTTVT-DTTPD/$PC_{71}BM$ blend films prepared with or without the DIO additive.

The morphologies of the blend films prepared using a mixed solvent containing chlorobenzene and 3% DIO were much more uniform with minimal phase separation, indicating good miscibility between the donor polymer and the PCBM acceptor. These factors may have led to increases in the J_{sc} value.

The EQE values (which were measured to evaluate the photoresponses of the fabricated solar cells as a function of wavelength) are shown in Figure 6 for the PBDTT-DTTPD:$PC_{71}BM$ and PBDTTVT-DTTPD:$PC_{71}BM$ devices prepared with or without the DIO additive. The PBDTT-DTTPD and PBDTTVT-DTTPD devices yielded an EQE plot that was similar to the absorption spectra of their PCBM blend films, indicating that excitons were mainly generated in the polymer phase (Figure S6). In Figure S6, the absorption coefficients of PBDTTVT-DTTPD/PCBM film showed higher values than those of PBDTT-DTTPD/PCBM film at 350−800 nm, which correlates with higher EQE values of PBDTTVT-DTTPD/PCBM device. The spectral response of the PBDTT-DTTPD/PCBM (1:1) + DIO device revealed that photons of wavelength 350−700 nm contributed significantly to the EQE, with a maximum EQE of 59% at 480 nm. The PBDTTVT-DTTPD/PCBM (1:1) + DIO device exhibited a similar spectral response in the range 350−700 nm; however, a maximum EQE of 71% was obtained at 480 nm, which resulted in a much higher J_{sc} of 10.9 mA/cm^2.

CONCLUSION

In conclusion, we report the facile synthesis and characterization of a new conjugated polymer comprising a DTTPD acceptor and a BDT donor bearing highly conjugated alkyl thienylenevinylene thiophene (TVT) side groups. We found that the conjugated TVT side groups in PBDTTVT-DTTPD play a crucial role in the absorption spectra, energy levels, charge transport, blend film morphology, and photovoltaic properties of the polymer. Our preliminary results indicate that the BDT donor units containing conjugated TVT side groups have significant potential as building blocks for conjugated polymers for OPVs.

dx.doi.org/10.1021/ma402245t | Macromolecules 2014, 47, 97−105

EXPERIMENTAL SECTION

Instrumentation. ^{1}H and ^{13}C NMR spectra were recorded on Bruker AVANCE 400 spectrometer, with tetramethylsilane as an internal reference. Elemental analysis was done by using PerkinElmer 2400 Series II CHNS/O analyzer. Fast atom bombardment (FAB) mass spectra were recorded on a JEOL, JMS-AX505WA, HP5890 series II. The optical absorption spectra were measured by a shimadzu UV-3100 UV−vis−NIR spectrometer. The number- and weight-average molecular weights of polymers were determined by gel permeation chromatography (GPC) on a Viscotek T60A instrument, using chloroform as eluting solvent and polystyrene as standard. The differential scanning calorimetry (DSC) and thermal gravimetric analysis (TGA) were made using a TA Q100 instrument and operated under a nitrogen atmosphere. Cyclic voltammetry (CV) was performed on an AUTOLAB/PG-STAT12 model system with a three-electrode cell in a solution of Bu_4NBF_4 (0.10 M) in acetonitrile at a scan rate of 50 mV/s. Polymer film coatings on ITO anode electrode were formed by the spin-coating method. Atomic force microscopy (AFM) was measured by tapping-mode using Multimode IIIa, Digital Instruments.

Materials. Compound **3**,[17] compound **7**,[18] and compound **8**[19] were synthesized according to previously published procedures.

Compound 1. Into a solution of thiophene (5.0 g, 0.059 mol) in THF (60 mL) at −78 °C was added, by syringe, 40.0 mL (0.071 mol) of *n*-butyllithium (1.6 M in *n*-hexane). The mixture was stirred at −78 °C for 30 min, and then 2-ethylhexyl bromide (9.3 mL, 0.049 mol) was added to the mixture. After the addition, the reaction mixture was heated at 80 °C for 12 h. The reaction mixture was poured into the water, extracted with $CHCl_3$, and dried with anhydrous $MgSO_4$. The solvent was removed via rotary evaporation, and the residue was purified by vacuum distillation to give a colorless liquid. (5.5 g, 49%). ^{1}H NMR ($CDCl_3$, 300 MHz, ppm): δ 7.06 (s, 1H) 7.04 (d, 1H), 6.80 (d, 1H), 2.74 (d, 2H), 1.56 (m, 1H), 1.28−1.27 (m, 8H), 0.88 (t. 6H). ^{13}C NMR ($CDCl_3$, 75 MHz, ppm): δ 111.00, 14.32, 23.22, 25.71, 29.07, 32.56, 34.02, 41.67, 76.80, 77.22, 77.65, 123.07, 125.11, 126.67, 144.41.

Compound 2. In a 500 mL flask, 11.0 mL of dimethylformamide (DMF) and 4.0 g of compound **1** (0.018 mol) were mixed and stirred at 0 °C for 10 min. 8.5 mL of $POCl_3$ (0.089 mol) was added slowly to the reaction mixture. The mixture was stirred at 85 °C for 2 h and then poured into water, neutralized with sodium bicarbonate, extracted with $CHCl_3$, and dried with anhydrous $MgSO_4$. The solvent was removed via rotary evaporation, and the residue was purified by vacuum distillation to give a colorless liquid (4.0 g, 89%). ^{1}H NMR ($CDCl_3$, 300 MHz, ppm): δ 9.81 (s, 1H) 7.60 (d, 1H), 6.89 (d, 1H), 2.79 (d, 2H), 1.32 (m, 1H), 1.29−1.27 (m, 8H), 0.89 (t. 6H). ^{13}C NMR ($CDCl_3$, 75 MHz, ppm): δ 10.88, 14.20, 23.04, 25.65, 28.89, 32.46, 34.93, 41.57, 76.81, 77.23, 77.65, 126.95, 137.09, 141.92, 156.64, 182.70. Mass (Fab); (m/z): 225 (M^+). Anal. Calcd for $C_{13}H_{20}OS$: C, 69.59; H, 8.98; O, 7.13; S, 14.29. Found: C, 69.97; H, 8.93; S, 13.98.

Compound 4. 14.2 mL (0.014 mol) of potassium *tert*-butoxide (1.0 M in THF) was added dropwise to the solution of compound **2** (3.0 g, 0.011 mol) and compound **3** (3.3 g, 0.014 mol) in THF (30 mL) at 0 °C. The mixture was stirred at RT for 2 h. The mixture was poured into water, extracted with $CHCl_3$, and dried with anhydrous $MgSO_4$. The solvent was removed via rotary evaporation, and the residue was purified with column chromatography on silica gel with hexane as eluent to give a pale yellow solid (3.5 g, 91%). ^{1}H NMR ($CDCl_3$, 300 MHz, ppm): δ 7.13 (d, 1H) 7.00−6.88 (m, 4H), 6.82 (d, 1H), 6.62 (d, 1H), 2.71 (d, 2H), 1.59−1.50 (m, 1H), 1.29−1.28 (m. 8H) 0.88 (t, 6H). ^{13}C NMR ($CDCl_3$, 75 MHz, ppm): δ 11.04, 14.35, 23.20, 25.71, 29.07, 32.57, 34.54, 41.56, 76.81, 77.23, 77.65, 120.34 122.17, 124.02, 125.67, 125.90, 126.28, 127.76, 140.33, 142.90, 144.26 Mass (Fab); (m/z): 304 (M^+). Anal. Calcd for $C_{18}H_{24}S_2$: C, 71.00; H, 7.94; S, 21.06 Found: C, 70.65; H, 8.14; S, 20.44.

Compound 5. Into a solution of compound **4** (3.0 g, 9.0 mmol) in THF (25 mL) at −40 °C was added, by syringe, 4.8 mL (9.62 mmol) of lithium diisopropylamide (LDA, 2.0 M in THF). The mixture was stirred at −40 °C for 30 min and allowed to warm to 0 °C, and then benzo[1,2-*b*:4,5-*b*′]dithiophene-4,8-dione (0.66 g, 3.0 mmol) was added. After the addition, the reaction mixture was heated at 50 °C for 2 h. The reaction mixture was cooled to 0 °C, and tin chloride dihydrate (4.5 g) dissolved in 10 mL of HCl was added. The mixture was stirred at room temperature for 1 h and then quenched with water. The mixture was extracted with $CHCl_3$ and dried with anhydrous $MgSO_4$. The solvent was removed via rotary evaporation, and the residue was purified with column chromatography on silica gel with hexane and $CHCl_3$ (4:1 [v/v]) as eluent to give a yellow solid. (0.76 g, 30%). ^{1}H NMR ($CDCl_3$, 300 MHz, ppm): δ 7.70 (d, 2H) 7.58 (d, 2H), 7.35 (d, 2H), 7.14 (d, 2H), 7.04 (d, 2H), 6.95 (d, 2H), 6.88 (d. 2H) 6.65 (d, 2H) 2.75 (d, 4H), 1.54 (m, 2H), 1.34 (m, 18H), 0.89 (t,12H). ^{13}C NMR ($CDCl_3$, 75 MHz, ppm): δ 8.04, 0.22, 11.09, 14.37, 23.22, 25.78, 29.12, 32.63, 34.64, 41.63, 120.30, 122.61, 126.04, 126.55, 128.97, 131.15, 137.57, 140.42, 143.14, 143.69, 144.64. Mass (Fab); (m/z): 794 (M^+). Anal. Calcd for $C_{46}H_{50}S_6$: C, 69.47; H, 6.34; S, 24.19. Found: C, 69.78; H, 6.25; S, 23.74.

Compound 6. Compound **5** (0.7 g, 0.82 mmol) was dissolved in 50 mL of dry THF at −78 °C for 1h under a nitrogen atmosphere, then 0.94 mL of LDA (1.89 mmol, 2.0 M in THF) was added dropwise. The reaction was stirred at −78 °C for 1 h, then 2.05 mL of trimethyltin chloride (2.05 mmol, 1.0 M in THF) was added to the reaction mixture. The reaction was stirred at −78 °C for 15 min and was allowed to warm to room temperature. The mixture was poured into water, extracted with $CHCl_3$, dried with anhydrous $MgSO_4$. The solvent was removed via rotary evaporation, and the residue was precipitated with $CHCl_3$ and methanol to yield pale yellow solid (0.82 g, 85%) ^{1}H NMR ($CDCl_3$, 300 MHz, ppm): δ 7.70 (s, 2H), 7.39 (d, 2H), 7.14 (d, 2H), 7.02 (d, 2H), 6.97 (d, 2H), 6.88 (d, 2H), 6.65 (d, 2H) 2.76 (d, 4H), 1.31 (m, 16H) 0.90 (t, 12H), 0.41(t, 18H). ^{13}C NMR ($CDCl_3$, 75 MHz, ppm): δ 11.08, 14.37, 23.22, 25.78, 29.12, 32.63, 34.64, 41.63, 76.81, 77.23, 77.65, 120.29, 122.35, 122.60, 126.04, 126.21, 126.55, 128.97, 131.14, 137.56, 138.98, 140.42 143.13, 143.54, 143.69, 144.63. Mass (Fab); (m/z): 1120 (M^+) Anal. Calcd for $C_{52}H_{66}S_6Sn_2$: C, 55.72; H, 5.93; S, 17.16; Sn, 21.18. Found: C, 57.34; H, 6.07; S, 16.91.

PBDTT-DTTPD. Compound **7** (0.200 g, 0.264 mmol), compound **8** (0.215 g, 0.277 mmol), and tetrakis(triphenylphosphene)palladium(0) (9.0 mg, 7.94×10^{-3} mmol) were dissolved in toluene (10.0 mL) and DMF (1.0 mL) under a nitrogen atmosphere. The reaction mixture was heated at 60 °C for 10 h. When the reaction had finished, the mixture was precipitated from the 10 mL of HCl and 150 mL of methanol. The polymer was dissolved in a small amount of $CHCl_3$ and precipitated in methanol. The resulting polymer was further purified by Soxhlet extraction using methanol, acetone, and hexane and then dried in a vacuum to give dark solid (0.18 g, yield 62%). Anal. Calcd for $(C_{63}H_{89}NO_4S_5)_n$: C, 69.76; H, 8.27; N, 1.29; O, 5.90; S, 14.78. Found: C, 68.79; H, 7.96; N, 1.33; S, 15.32.

PBDTTVT-DTTPD. Compound **6** (0.300 g, 0.255 mmol), compound **8** (0.183 g, 0.242 mmol), and tetrakis(triphenylphosphene)-palladium(0) (8.8 mg, 7.64×10^{-3} mmol) were dissolved in toluene (10.0 mL) and DMF (1.0 mL) under a nitrogen atmosphere. The reaction mixture was heated at 60 °C for 10 h. When the reaction had finished, the mixture was precipitated from the 10 mL of HCl and 150 mL of methanol. The polymer was dissolved in a small amount of $CHCl_3$ and precipitated in methanol. The resulting polymer was further purified by Soxhlet extraction using methanol, acetone, and hexane and then dried in a vacuum to give dark solid (0.32 g, yield 98%). Anal. Calcd for $(C_{78}H_{91}NO_2S_9)_n$: C, 68.73; H, 6.73; N, 1.03; O, 2.35; S, 21.17. Found: C, 68.60; H, 6.75; N, 1.01; S, 20.91.

Fabrication of the Organic Field-Effect Transistors (OFETs). OFET devices were fabricated in a bottom-contact geometry (channel length = 12 μm, width = 120 μm). The source and drain contacts consisted of gold (100 nm), and the dielectric was silicon oxide (SiO_2) with a thickness of 300 nm. The SiO_2 surface was cleaned, dried, and pretreated with a solution of 1.0 mM octyltrichlorosilane (OTS-8) in toluene at room temperature for 2 h under nitrogen to produce nonpolar and smooth surfaces onto which the polymers could be spin-coated. The polymers were dissolved to a concentration of 0.5 wt % in chloroform. Films of the organic semiconductors were spin-coated at

dx.doi.org/10.1021/ma402245t | *Macromolecules* 2014, 47, 97−105

1500 rpm for 50 s to a thickness of 50 nm, followed by an annealing process. All device fabrication procedures and measurements were carried out in air at room temperature. Electrical characteristics of the TFTs were measured in ambient conditions using both Keithley 2400 and 236 source/measure units.

Fabrication of Hole-Only Devices. The hole mobilities of the PBDTT-DTTPD and PBDTTVT-DTTPD films were determined by employing the space-charge limited current (SCLC) model to the $J-V$ measurement of the device. The hole-only devices were fabricated with the structure ITO/PEDOT:PSS/polymers/Au. The hole mobilities of the fabricated devices were calculated from the space charge limited current (SCLC) by the equation

$$J_{SCLC} = (9/8)\varepsilon_r\varepsilon_0\mu(V^2/L^3)$$

where ε_r is the dielectric constant of the polymer layer, ε_0 is permittivity of free space, μ is the SCLC mobility, L is the distance between the cathode and anode, which is equivalent to the film thickness, and V is the applied voltage.

Fabrication of the Polymer Solar Cells (PSCs). In this study, the devices were fabricated with the structure ITO/PEDOT:PSS/polymer:$PC_{71}BM$/LiF/Al. The procedure for cleaning the ITO surface included sonication and rinsing in deionized water, methanol, and acetone. The hole-transporting PEDOT:PSS layer was spin-coated onto each ITO anode from a solution purchased from Heraeus (CleviosTM P VP AI4083) and baked for 20 min at 140 °C in glovebox. Each polymer:$PC_{71}BM$ solution was then spin-coated onto the PEDOT:PSS layer. The polymer solution for spin-coating was prepared by dissolving the polymer (1 wt %) in chlorobenzene. Preannealing was not carried out. LiF and aluminum contacts were formed by vacuum deposition at pressures below 3×10^{-6} Torr, providing an active area of 0.09 cm^2. Solar cell efficiencies were characterized under simulated 100 mW/cm^2 AM 1.5G irradiation from a Xe arc lamp with an AM 1.5 global filter. Simulator irradiance was characterized using a calibrated spectrometer, and the illumination intensity was set using an NREL certified silicon diode with an integrated KG1 optical filter. The EQE was measured by underfilling the device are a using a reflective microscope objective to focus the light output from a 100 W halogen lamp outfitted with a monochromator and optical chopper; the photocurrent was measured using a lock-in amplifier, and the absolute photon flux was determined using a calibrated silicon photodiode. All device fabrication procedures and measurements were carried out in air at room temperature.

■ ASSOCIATED CONTENT

Supporting Information

DSC, TGA, CV, computation, and SCLC results of the polymers. This material is available free of charge via the Internet at http://pubs.acs.org.

■ AUTHOR INFORMATION

Corresponding Author

*E-mail inamkang@catholic.ac.kr (I.-N.K.).

Author Contributions

H.-S.C. and W.-H.L. contributed equally in this work.

Notes

The authors declare no competing financial interest.

■ ACKNOWLEDGMENTS

This study was supported by a grant from the cooperative R&D Program (B551179-08-03-00) funded by the Korea Research Council Industrial Science and Technology, Republic of Korea and also supported by New and Renewable Energy Program of the Korea Institute of Energy Technology Evaluation and Planning (KETEP) funded by the Korea government Ministry of Trade, industry & Energy (20113010010030).

■ REFERENCES

(1) Søndergaard, R. R.; Hosel, M.; Krebs, F. C. *J. Polym. Sci., Part B: Polym. Phys.* **2013**, *51*, 16.

(2) (a) Kim, J.-H.; Song, C. E.; Kang, I.-N.; Shin, W. S.; Hwang, D.-H. *Chem. Commun.* **2013**, *49*, 3248. (b) Cabanetos, C.; Labban, A. E.; Bartelt, J. A.; Douglas, J. D.; Mateker, W. R.; Frechet, J. M. J.; McGehee, M. D.; Beaujuge, P. M. *J. Am. Chem. Soc.* **2013**, *135*, 4656. (c) Lee, W.-H.; Son, S.-K.; Kim, K.; Lee, S. K.; Shin, W.-S.; Moon, S.-J.; Kang, I.-N. *Macromolecules* **2012**, *45*, 1303.

(3) Dou, L.; You, J.; Yang, J.; Chen, C.-C.; He, Y.; Murase, S.; Moriarty, T.; Emery, K.; Li, G.; Yang, Y. *Nat. Photonics* **2012**, *6*, 180.

(4) (a) Perzon, E.; Zhang, F.; Andersson, M.; Mammo, W.; Inganas, O. A.; Andersson, M. R. *Adv. Mater.* **2007**, *19*, 3308. (b) Jespersen, K. G.; Beenken, W. J. D.; Zaushitsyn, Y.; Yartsev, A.; Andersson, M.; Pullerits, T.; Sundstrom, V. *J. Chem. Phys.* **2004**, *121*, 12613. (c) Gadisa, A.; Mammo, W.; Andersson, L. M.; Admassie, S.; Zhang, F.; Andersson, M. R.; Inganas, O. *Adv. Funct. Mater.* **2007**, *17*, 3836.

(5) (a) Price, S. C.; Stuart, A. C.; Yang, L.; Zhou, H.; You, W. *J. Am. Chem. Soc.* **2011**, *133*, 4625. (b) Zhou, H.; Yang, L.; Stuart, A. C.; Price, S. C.; Liu, S.; You, W. *Angew. Chem., Int. Ed.* **2011**, *50*, 2995. (c) Liang, Y.; Xu, Z.; Xia, J.; Tsai, S.-T.; Wu, Y.; Li, G.; Ray, C.; Yu, L. *Adv. Mater.* **2010**, *22*, E135. (d) Liang, Y.; Feng, D.; Wu, Y.; Tsai, S.-T.; Li, G.; Ray, C.; Yu, L. *J. Am. Chem. Soc.* **2009**, *131*, 7792. (e) Zhang, G.; Fu, Y.; Zhang, Q.; Xie, Z. *Chem. Commun.* **2010**, *46*, 4997. (f) Zhang, M.; Fan, H.; Guo, X.; He, Y.; Zhang, Z.-G.; Min, J.; Zhang, J.; Zhao, G.; Zhan, X.; Li, Y. *Macromolecules* **2010**, *43*, 8714. (g) Zou, Y.; Najari, A.; Berrouard, P.; Beaupre, S.; Reda, A. B.; Tao, Y.; Leclerc, M. *J. Am. Chem. Soc.* **2010**, *132*, 5330. (h) Piliego, C.; Holcombe, T. W.; Douglas, T. J.; Woo, C. H.; Beaujuge, P. M.; Frechet, J. M. J. *J. Am. Chem. Soc.* **2010**, *132*, 7595.

(6) (a) Kim, H. G.; Jo, S. B.; Shim, C.; Lee, J.; Shin, J.; Cho, E. C.; Ihn, S.-G.; Choi, Y. S.; Kim, Y.; Cho, K. *J. Mater. Chem.* **2012**, *22*, 17709. (b) Shi, Q.; Fan, H.; Liu, Y.; Hu, W.; Li, Y.; Zhan, X. *Macromolecules* **2011**, *44*, 9173. (c) Huo, L.; Guo, X.; Zhang, S.; Li, Y.; Hou, J. *Macromolecules* **2011**, *44*, 4035. (d) Wang, M.; Hu, X.; Liu, P.; Li, W.; Gong, X.; Huang, F.; Cao, Y. *J. Am. Chem. Soc.* **2011**, *133*, 9638. (e) Duan, R.; Ye, L.; Guo, X.; Huang, Y.; Wang, P.; Zhang, S.; Zhang, J.; Huo, L.; Hou, J. *Macromolecules* **2012**, *45*, 3032. (f) Kularatne, R. S.; Sista, P.; Nguyen, H. Q.; Bhatt, M. P.; Biewer, M. C.; Stefan, M. C. *Macromolecules* **2012**, *33*, 9. (g) Min, J.; Zhang, Z.-G.; Zhang, S.; Li, Y. *Chem. Mater.* **2012**, *24*, 3247.

(7) (a) Huo, L.; Zhang, S.; Guo, X.; Xu, F.; Li, Y.; Hou, J. *Angew. Chem., Int. Ed.* **2011**, *50*, 9697. (b) Wang, M.; Hu, X.; Liu, P.; Li, W.; Gong, X.; Huang, F.; Cao, Y. *J. Am. Chem. Soc.* **2011**, *133*, 9638. (c) Li, W.; Roelofs, W. S. C.; Wienk, M. M.; Janssen, R. A. J. *J. Am. Chem. Soc.* **2012**, *134*, 13787. (d) Huo, L.; Hou, J.; Zhang, S.; Chen, H.-Y.; Yang, Y. *Angew. Chem., Int. Ed.* **2010**, *49*, 1500.

(8) Kularatne, R. S.; Sista, P.; Nguyen, H. Q.; Bhatt, M. P.; Biewer, M. C.; Stefan, M. C. *Macromolecules* **2012**, *45*, 7855.

(9) (a) Hou, J.; Tan, Z.; He, Y.; Yang, C.; Li, Y. *Macromolecules* **2006**, *39*, 4657. (b) Hou, J.; Tan, Z.; Yan, Y.; He, Y.; Yang, C.; Li, Y. *J. Am. Chem. Soc.* **2006**, *128*, 4911.

(10) Peverati, R.; Truhlar, D. G. *Phys. Chem. Phys. Chem.* **2012**, *14*, 16187.

(11) Frisch, M. J.; Trucks, G. W.; Schlegel, H. B.; Scuseria, G. E.; Robb, M. A.; Cheeseman, J. R.; Scalmani, G.; Barone, V.; Mennucci, B.; Petersson, G. A.; Nakatsuji, H.; Caricato, M.; Li, X.; Hratchian, H. P.; Izmaylov, A. F.; Bloino, J.; Zheng, G.; Sonnenberg, J. L.; Hada, M.; Ehara, M.; Toyota, K.; Fukuda, R.; Hasegawa, J.; Ishida, M.; Nakajima, T.; Honda, Y.; Kitao, O.; Nakai, H.; Vreven, T.; Montgomery, J. A.; Peralta, J. E.; Ogliaro, F.; Bearpark, M.; Heyd, J. J.; Brothers, E.; Kudin, K. N.; Staroverov, V. N.; Kobayashi, R.; Normand, J.; Raghavachari, K.; Rendell, A.; Burant, J. C.; Iyengar, S . S.; Tomasi, J.; Cossi, M.; Rega, N.; Millam, J. M.; Klene, M.; Knox, J. E.; Cross, J. B.; Bakken, V.; Adamo, C.; Jaramillo, J.; Gomperts, R.; Stratmann, R. E.; Yazyev, O.; Austin, A. J.; Cammi, R.; Pomelli, C.; Ochterski, J. W.; Martin, R. L.; Morokuma, K.; Zakrzewski, V. G.; Voth, G. A.; Salvador, P.; Dannenberg, J. J.; Dapprich, S.; Daniels, A. D.; Farkas, Ö.;

Foresman, J. B.; Ortiz, J. V.; Cioslowski, J.; Fox, D. J. *Gaussian 09, Revision D.01*; Gaussian, Inc.: Wallingford, CT, 2009.
(12) Dimitrakoupoulos, C. D.; Melenfant, R. M. *Adv. Mater.* **2002**, *14*, 99.
(13) Kim, K.-H.; Kang, H.; Kim, H. J.; Kim, P. S.; Yoon, S. C.; Kim, B. *Chem. Mater.* **2012**, *24*, 2373.
(14) Scharber, M. C.; Mühlbacher, D.; Koppe, M.; Denk, P.; Waldauf, C.; Heeger, A. J.; Brabec, C. J. *Adv. Mater.* **2006**, *18*, 789.
(15) (a) Li, Y.; Xu, B.; Li, H.; Cheng, W.; Xue, L.; Chen, F.; Lu, H.; Tian, W. *J. Phys. Chem. C* **2011**, *115*, 2386. (b) Chen, H.-Y.; Hou, J.; Zhang, S.; Liang, Y.; Yang, G.; Yang, Y.; Yu, L.; Wu, Y.; Li, G. *Nat. Photonics* **2009**, *3*, 649.
(16) Halls, J. J. M.; Pichler, K.; Friend, R. H.; Moratti, S. C.; Holmes, A. B. *Appl. Phys. Lett.* **1996**, *68*, 3120.
(17) Lee, W.-H.; Kong, H.; Oh, S.-Y.; Shim, H.-K.; Kang, I.-N. *J. Polym. Sci., Part A: Polym. Chem.* **2009**, *47*, 111.
(18) Huo, L.; Ye, L.; Wu, Y.; Li, Z.; Guo, X.; Zhang, M.; Zhang, S.; Hou, J. *Macromolecules* **2012**, *45*, 6923.
(19) Najari, A.; Beaupre, S.; Berrouard, P.; Zou, Y.; Pouliot, J.-R.; Lepage-Perusse, C.; Leclerc, M. *Adv. Funct. Mater.* **2011**, *21*, 718.